Tissue heterogeneity is associated with phenotypic but not genomic diversity in *Wolbachia* endosymbionts

Romain Pigeault[1*], Yann Dussert[1], Raphaël Jorge[3,4], Theo Ulve[1], Marie Panza[1], Maryline Raimond[1], Carine Delaunay[1], Willy Aucher[1], Thierry Berges[1], David Ogereau[5], Bouziane Moumen[1], Jean Peccoud[1†], Richard Cordaux[5†]

[1] Université de Poitiers, CNRS, EBI, UMR 7267, Poitiers, France

[2] Génomique Métabolique, Genoscope, Institut François Jacob, CEA, CNRS, Univ Evry, Université Paris-Saclay, Evry, 91057, France

[3] Université Lyon 1, CNRS, VetAgroSup, Laboratoire de Biométrie et Biologie Evolutive, UMR 5558, Villeurbanne, France

[4] INSA Lyon, INRAE, Biologie fonctionnelle, insectes et interactions, UMR203, Villeurbanne, France

[5] Université Paris-Saclay, CNRS, IRD, UMR Évolution Génomes Comportement Écologie, 91190 Gif-sur-Yvette, France

ORCID :

Romain Pigeault: 0000-0002-8011-4600

Yann Dussert: 0000-0003-1900-7715

David Ogereau : 0000-0002-4496-3007

Bouziane Moumen: 0000-0002-1789-6160

Jean Peccoud: 0000-0002-3356-7869

Richard Cordaux: 0000-0003-4997-735X

*Corresponding author: **Romain Pigeault -** romain.pigeault@univ-poitiers.fr

[†] Jean Peccoud and Richard Cordaux share senior authorship

Running Head: *Wolbachia* within-host diversity

Abstract

The mechanisms underlying within-host diversification in parasite populations are poorly understood. Yet, phenotypic and genotypic variation in parasites can shape their evolutionary trajectories and have important epidemiological consequences. Our aim was to determine whether the constraints associated with infecting different host tissues lead to the emergence and coexistence of multiple parasite sub-populations with distinct phenotypes. We tested this hypothesis using the most widespread bacterial endosymbiont, *Wolbachia*. We injected *Wolbachia* bacteria isolated from three tissues of the common pill-bug (*Armadillidium vulgare*) into uninfected individuals and monitored the growth rate and virulence of each bacterial sub-population in the new hosts. Our results highlight that within-host tissue heterogeneity leads to diverse *Wolbachia* phenotypes. High-depth genome re-resequencing of *Wolbachia* sub-populations revealed that this polymorphism was not due to genomic variation but was more likely a result of phenotypic plasticity. Indeed, we found no recurrent tissue-specific genomic variation among infected individuals. Our single nucleotide polymorphism (SNP) filtration pipeline, developed to ensure SNP validity, detected only one substitution. This *Wolbachia* variant, observed in one female, was present in all three bacterial sub-populations, with frequencies ranging from 24% to 58% depending on the tissue. Overall, our results support the stability of the *Wolbachia* genome with respect to the rarity of point mutations, in agreement with reports from other symbiotic systems. From a methodological perspective, our study highlights the need for considerable caution when detecting variants in endosymbiont populations, as our conservative approach led us to exclude more than 99.5% of the initially called variants.

Keywords: adaptation, acclimation, feminizing *Wolbachia*, infection dynamics, subpopulation, tissue tropism, variant calling, within-host evolution

1. Introduction

Among the many factors that influence species richness and community structure, environmental heterogeneity is generally considered to be a particularly important driver (Ben-Hur & Kadmon, 2020; Stein et al., 2014; Stein & Kreft, 2015). Since heterogeneous environments offer a variety of ecological niches and refuges from adverse conditions, species richness and persistence should increase with greater spatial heterogeneity (Ben-Hur & Kadmon, 2020; Burnett et al., 1998; Stein et al., 2014; Yang et al., 2015). Environmental heterogeneity also promotes genetic and phenotypic diversity within species through diversifying selection (Houle et al., 2020; B.-H. Huang et al., 2017; Mcdonald & Ayala, 1974; Rainey & Travisano, 1998), which may underpin local adaptations (Y. Huang et al., 2016; Qian et al., 2024; Trevail et al., 2021; van Houte et al., 2021). However, most studies that investigated relationships between environmental heterogeneity and diversity have focused on free-living species (e.g., (Langenheder & Lindström, 2019; Stein & Kreft, 2015)). The relationship between environmental heterogeneity and both endoparasites species diversity and phenotypic variability remains underexplored.

For endoparasites, environmental heterogeneity can exist both within individual hosts and across different hosts. Variation among individuals within host population is known to shape parasite evolution (Johnson et al., 2016; Regoes et al., 2000; White et al., 2020), driving rapid diversification (Johnson et al., 2016; Kamiya et al., 2014). However, a single host individual is treated by most theoretical and empirical studies on endoparasite evolution as a homogeneous environment – a single population of target cells without any structure – neglecting heterogeneities in cell type, immune response, nutrient supply or microbiota composition. Yet, several parasites exploit a heterogeneous environment composed of

different biological tissues and fluids which form a spatially structured fitness landscape for the parasite. Successful colonization of different microenvironments, with their contrasted constraints, may involve the expression or selection of different parasitic phenotypes leading to within-host differentiation into several sub-populations (Didelot et al., 2016). This phenotypic variability can reflect phenotypic plasticity (e.g., expression plasticity, (Wernegreen & Wheeler, 2009), selection of genetic variants initially present in the inoculum (Chrostek & Teixeira, 2018) or of new variants arising from spontaneous mutations (Ailloud et al., 2019).

The co-occurrence of polymorphic sub-populations of parasites in different tissues or cell types has been described in several biological models. RNA viruses (e.g., plum pox virus, influenza, SARS-CoV-2, poliovirus) may display genetic diversity within single infected hosts, and co-existing viral variants may evolve differently in distinct cell types (Gupta et al., 2022; Jridi et al., 2006; Xiao et al., 2017). The ability of some RNA viruses to adapt to tissue-specific innate immune microenvironments may actually be critical for establishing robust infections (Xiao et al., 2017). Gastric biopsies from multiple stomach regions of *Helicobacter pylori*-infected hosts showed location-specific evolution of the bacteria, suggesting the existence of structured niches with distinct selective pressures within the stomach (Ailloud et al., 2019). In other cases, such as *Pseudomonas aeruginosa* or *Mycobacterium tuberculosis* chronic infections, the emergence of polymorphic sub-populations seems to be driven by tissue-specific adaptation (Jorth et al., 2015; Lieberman et al., 2016). Some within-host parasite sub-populations may constitute a reservoir from which new virulent variants can emerge (Bessière & Volmer, 2021), and which can delay clearance of parasite infection by the host immune system or drugs (Avettand-Fenoel et al., 2011; Clement et al., 2005; Obaldia et al., 2018). Understanding the evolutionary forces and mechanisms at the origin of within-host parasite

diversity is essential, yet it is rarely studied. Descriptive studies (e.g., long-term ambulatory monitoring of chronically infected patients) cannot trace the divergence of variants found within a host and cannot identify the drivers of their diversification without controlling or assessing the composition of the infectious inoculum and ensuring the absence of subsequent infections. For this purpose, vertically transmitted parasites are particularly useful, as their transmission mode ensures the common origin of all within-host parasite sub-populations.

Among the most widespread vertically transmitted endosymbionts in animals is *Wolbachia pipientis*. This primarily maternally transmitted intracellular alpha-proteobacterium is widely distributed among arthropods and has been extensively studied with respect to its peculiar effects on its hosts (Kaur et al., 2021; LePage & Bordenstein, 2013). *Wolbachia* manipulates host reproduction in various ways, including the feminization of chromosomal male embryos, parthenogenesis, male killing, and sperm–egg incompatibility (Werren et al., 2008)). This endosymbiont can also have positive or negative effects on other aspects of the host's life cycle (e.g., immunity, senescence) and influence the evolution of the host genome through horizontal gene transfer (Cordaux & Gilbert, 2017; Depeux et al., 2024; Sicard et al., 2014). The diversity of effects of *Wolbachia* on its hosts certainly relates to its wide distribution within infected individuals (Sicard et al., 2014). In addition to colonizing the female germline, ensuring vertical transmission, *Wolbachia* has indeed been observed in all major tissues (e.g., nerve chain, immune and digestive compartments, (Pietri et al., 2016)) of many arthropod species. The presence of vertically transmitted endosymbionts in somatic tissues may seem paradoxical, especially considering that systemic infection can decrease host fitness. Given this disadvantage (i.e., fitness alignment), these extensive somatic localizations must somehow benefit the parasite. Localization of *Wolbachia* in somatic tissues could influence host biology in such a way that favours its vertical and, possibly, horizontal

121 transmission. However, the ability of the bacteria to colonize and establish in different tissular
122 microenvironments could involve the expression or selection of different phenotypes.

123 To investigate this hypothesis, we assessed the relationship between tissue
124 environment heterogeneity and phenotype variability in the *w*VulC *Wolbachia* strain, which
125 infects the common pill-bug *Armadillidium vulgare* (Cordaux et al., 2004). We focused on three
126 naturally infected tissues, which we selected for their physiological characteristics and the
127 benefits that *Wolbachia* could gain by colonizing them: (i) gonads, which are a prime target
128 for vertical transmission, (ii) haemocytes, as these circulating immune cells could contribute
129 to spread *Wolbachia* to different host tissues and may facilitate its horizontal transmission
130 (Braquart-Varnier et al., 2015), and (iii) the nerve chain, as the localization of *Wolbachia* in the
131 brain and nerve chord could induce adaptive modifications of host behaviour (Bi & Wang,
132 2020; Templé & Richard, 2015). We hypothesized that the main phenotypic variation between
133 bacteria sub-populations colonizing these tissues pertained to their replication rate. A high
134 replication rate in vital tissues, such as the nerve chain, could disrupt tissue structure and
135 reduce host lifespan (Le Clec'h et al., 2012; Strunov & Kiseleva, 2016). Thus, we expected
136 *Wolbachia* populations from the host nerve system to show lower replication rates than those
137 from the other tissues. We tested this hypothesis by injecting *Wolbachia* extracted from the
138 three tissue types into uninfected *A. vulgare* individuals, and by monitoring their growth rates
139 in their new hosts. We then tested whether *Wolbachia* sub-populations were adapted and not
140 merely acclimated to their tissue types. In this case, we expected to find recurrent tissue-
141 specific genomic variation among infected individuals. We tested this prediction by
142 sequencing the whole genomes of focal bacterial sub-populations.

2. Materials and Methods

2.1 Biological models

All *A. vulgare* individuals used in this experiment were reared as previously described (Sicard et al., 2010). Given that the *Wolbachia* strain used in this study is feminizing, all the individuals used were females. As *Wolbachia* is not cultivable, phenotyping sub-populations requires trans-infection of an uninfected host with bacterial isolates from naturally infected animals. For this purpose, we used a common pill-bug source line (WXw) infected by the *w*VulC *Wolbachia* strain (source individuals) and an uninfected recipient line (WXa, recipient individuals) into which we have injected bacteria. The two laboratory lines came from the same original population sampled in Helsingør (Denmark).

2.2 Experimental infection

To characterize the phenotype of the different *Wolbachia* sub-populations associated to three different tissues of their native host, five batches of trans-infection were carried out. Three batches (i.e., three biological replicates) were used to monitor early infection dynamics within the recipient host (day 0 to day 60 post-infection, trans-infection experiment 1), and two batches were used to estimate bacterial persistence in tissues (i.e., two biological replicates, day 200 post-infection, trans-infection experiment 2). For each batch, one tissue suspension was prepared from each of the following tissues: haemolymph, ovaries and nerve chain. Tissues were collected from five source females from the WXw line (infection status previously validated by quantitative PCR, see section 2.4). For each suspension, tissues were crushed in 1 mL of Ringer solution (1.4 mM CaCl2, 2.4 mM HNaCO3, 2 mM KCl, 0.4 M NaCl) for haemolymph and 2 mL for ovaries and nerve chain. The resulting suspension was filtered through a 1.2 µm pore membrane to remove cell debris and host cell nuclei. A prior

166 experiment conducted on 15 females from the source line (WXw) allowed us to highlight that
167 the number of bacteria per ng of DNA differed between the three target tissues (see **Fig. S1** in
168 appendix 1). Therefore, the filtered solutions were diluted in Ringer solution to adjust the final
169 concentration of bacteria at 2500 ± 300 cells/µL for the trans-infection batches used to
170 describe *Wolbachia* infection dynamics, and at 1282 ± 205 cells/µL for the two batches made
171 to investigate bacterial persistence 200 days after injection. The variation in *Wolbachia*
172 concentration between the two experiments stems from their differing timing, with the first
173 conducted in January and the second in April. Since *Wolbachia* concentration (number/ng of
174 DNA) can fluctuate based on host size and, consequently, age, this resulted in slight
175 differences in *Wolbachia* concentration between the two trans-infection experiments.
176 Another prior experiment showed that the proportion of live bacteria in the different filtered
177 tissue solutions was similar (LRT = 4.0279, p = 0.1335, proportion of live *Wolbachia* ± 95%CI,
178 haemolymph = 0.815 ± 0.017, nervous chain = 0.875 ± 0.014, ovaries = 0.862 ± 0.037, see
179 appendix 1 for a detailed protocol).

180 One µL of each filtrate was injected using a thin glass needle into the general cavity of
181 each recipient individual through a small hole pierced at its posterior part. Each tissue filtrate
182 from the three trans-infection batches used to study *Wolbachia* infection dynamics (trans-
183 infection experiment 1) was injected into 21 recipient females of the WXa line, resulting in a
184 total of 63 females transinfected per tissue filtrate. Then, on days 20, 40 and 60 post-injection,
185 6-7 recipient females per trans-infection batch were randomly selected to quantify *Wolbachia*
186 in the focal tissues (see section 2.4). To study bacterial persistence in recipient host tissues
187 (trans-infection experiment 2), 10 females were injected with each tissue filtrate for each of
188 the two trans-infection batches. Two hundred days post-injection, all surviving females were
189 dissected to quantify *Wolbachia* in the three focal tissues (see section 2.4). For each trans-

infection batch, control groups were created using the same protocol, but with female sources originating from the WXa line.

2.3 Mortality monitoring

The effect of *Wolbachia* injection on pill-bug mortality was monitored every 10 days as part of the study of the influence of *Wolbachia* tissue origin on the dynamics of early infection within the recipient host (trans-infection experiment 1), and every 15-25 days as part of the study of *Wolbachia* tissue origin on the persistence of the bacterium in tissues (trans-infection experiment 2). When individuals were harvested during the experiment to quantify *Wolbachia*, they were censored for the survival analysis (see section 2.9).

2.4 Quantification of *Wolbachia* in source and recipient host's tissues

To compare *Wolbachia* density in different tissues of source line and recipient hosts, total DNA was extracted from the haemolymph, nerve chain and ovaries of individuals using standard protocols (Qiagen DNeasy 96 Blood & Tissue kit). For each sample, the purity of the extracted DNA (OD 260/280 nm and 260/230 nm ratios) was measured using a Nanodrop 1000 spectrophotometer (Thermofisher). To quantify *Wolbachia* load, we developed a fluorescent probe-based quantitative PCR (qPCR) approach amplifying a *Wolbachia* locus and a reference host nuclear locus in the same reaction. We used primers wsp208f (5'- TGG-TGC-AGC-ATT-TAC-TCC-AG-3') and wsp413r (5'-TCG-CTT-GAT-AAG-CAA-AAC-CA-3') targeting the *Wolbachia* protein surface gene (*wsp*, (W. L. Le Clec'h et al., 2012)) and we designed primers amplifying a portion of the single-copy nuclear gene encoding the mitochondrial leucine-tRNA ligase of *A. vulgare*: TLeuF (5'- TGT-ACA-CAT-CGA-GCA-GCA-AG-3') and TLeuR (5'- AAA-GAG-GAG-CGG-AGA-GTT-TCA-G-3') (Durand et al., 2023). The *Wolbachia wsp* double-dye probe (5'-TTG-CAG-ACA-GTG-TGA-CAG-CGT-T-3') was labelled with Hexachlorofluorescein (HEX) as a reporter at the 5' end and Black Hole Quencher 1 (BHQ-1) at the 3' end. *A. vulgare* TLeu probe (5'-ACG-

AAG-TTC-GCC-CTG-TTC-TGG-A-3') was labelled with 6-carboxy-fluorescein (FAM) as a reporter and BHQ-1 as a quencher. The qPCR reactions were performed using Roche LIGHTCYCLER 480 with the following program: 2 min at 50°C, 10 min at 95°C and 45 cycles, 15 s at 95°C, and 1 min at 60°C. For each sample, two independent technical replicates were carried out and the mean cycle-threshold value was calculated. *Wolbachia* load was then calculated relative to the reference gene (TLeu) using the delate CP method: $2^{-(CP(wsp) - CP(TLeu))}$.

2.5 Genome assembly of *Wolbachia w*VulC

To study the within-host genetic diversity of *Wolbachia*, we first assembled the genome of the *w*VulC *Wolbachia* strain from the WXw line. Three female individuals were used for Oxford Nanopore Technologies (ONT) long-read sequencing and one for Illumina short-read sequencing. Total DNA from haemolymph, nerve chain and ovaries of each female was extracted using standard protocols (DNA used for ONT sequencing: Macherey-Nagel NucleoBond HMW DNA kit, DNA used for Illumina sequencing: Qiagen DNeasy 96 Blood & Tissue kit). The long-read sequencing library was prepared using the SQK-LSK109 Ligation Sequencing Kit (ONT) and sequenced with an R9.4.1 flow cell on a MinION Mk1B (ONT). Reads were basecalled with Guppy 6.3.8 (RRID:SCR_023196) using the SUP model. The short-read library was prepared using the TruSeq Nano DNA Library Prep kit (Illumina) and sequenced on a HiSeq X (Illumina, paired-end 2 × 150 bp).

ONT adapters were first trimmed with porechop 0.2.4 (https://github.com/rrwick/Porechop), and reads were filtered using NanoFilt 2.7.1 (minimum average quality: 7, minimum length: 1000 bp) implemented in NanoPack (De Coster et al., 2018). Reads were then assembled with Flye 2.8.3 (Kolmogorov et al., 2019) using default parameters. The entire assembly was first polished with the ONT reads using medaka 1.7 (https://github.com/nanoporetech/medaka, r941_min_fast_g507 model, 2 rounds). For

assembly polishing using short reads, Illumina reads were mapped onto the assembly with bwa-mem2 2.2.1 (Vasimuddin et al., 2019) and used for further polishing with Polypolish 0.4.3 (Wick & Holt, 2022). This step was carried out twice. The largest assembled contig was reported detected as circular by the Flye assembler and had the expected length (~1.6 Mb) of the *w*VulC *Wolbachia* genome. We aligned this contig against a previous version of the genome (GenBank accession: ALWU00000000.1) with nucmer in MUMmer 4.0.0rc1 (Marçais et al., 2018), confirming that the contig corresponded to the *w*VulC strain. After mapping the short reads for a third time onto this contig, short variants were called with Freebayes 1.3.1 (Garrison & Marth, 2012). Variants were then visually reviewed using the IGV genome browser (version 2.14.0) (Robinson et al., 2017). Eight of them, corresponding to errors, were kept. We corrected the genome sequence with these eight variants using the consensus command in BCFtools 1.17 (Danecek et al., 2021). Following the recommendations of Ioannidis (Ioannidis et al., 2007), the genome sequence was rotated to start at the *hemE* gene using the fixstart command of Circlator 1.5.5 (Hunt et al., 2015) . The genome was annotated with the NCBI Prokaryotic Genome Annotation Pipeline (PGAP) 2022-12-13.build6494 (Haft et al., 2024; Li et al., 2021; Tatusova et al., 2016). A search of Insertion Sequence (IS) elements was carried out with digIS v1.2 (Puterová & Martínek, 2021). Additionally, bacteriophage-derived regions were detected using PHASTEST (Wishart et al., 2023). Results of these annotations were plotted with Circos v0.69-9 (Krzywinski et al., 2009). The completeness of the genome and the gene annotation was assessed using BUSCO 5.3.2 (Manni et al., 2021) using the rickettsiales_odb10 dataset.

2.6 Whole-genome resequencing and variant calling

Three *A. vulgare* females from the WXw line were used to study the genetic diversity of the different *Wolbachia* sub-populations associated with the nerve chain, ovaries and

haemolymph. Two of these females were sisters (names: F1_2015 & F2_2015). The matriline of the third one (F_1999) diverged from the matriline of the sisters for 18 generations (i.e., 18 years). Females were dissected and their tissues isolated individually. Total DNA of each biological sample was extracted using the Qiagen DNeasy 96 Blood & Tissue kit. DNA purity and quantity were measured as described above. The haemolymph of two females could not be sequenced because it did not yield enough DNA. DNA libraries were prepared using the TruSeq Nano DNA Library Prep kit and sequenced on the Illumina HiSeq 2000 platform to generate 2×150 bp reads, by Genoscreen (Lille, France). Read quality was assessed with FastQC 0.11.9 (http://www.bioinformatics.babraham.ac.uk/projects/fastqc). Fastp 0.23.0 (Chen et al., 2018) was used to remove adapter contamination and systematic base calling errors. To mitigate misalignments of reads originating from the host genome, notably from *Wolbachia*-derived nuclear insertions (Chebbi et al., 2019; Leclercq et al., 2016), reads were aligned using bwa-mem2 (Vasimuddin et al., 2019) against a reference including our *w*VulC genome assembly, the assembly of the partial mitochondrial genome of *A. vulgare* (GenBank accession number: MF187614.1, (Peccoud et al., 2017)) and the genome assembly of *A. vulgare* (accession number: GCA_004104545.1, (Chebbi et al., 2019)). PCR duplicates were marked with samtools markdup (v1.14). Read coverage along the *w*VulC genome was computed for each sample for adjacent 5 kb windows using mosdepth 0.2.9 (Pedersen & Quinlan, 2018). For a given sample, normalized coverage for each window was calculated by dividing the coverage value by the median of all values in R (v. 4.2.1) (R Core Team, 2022). SNPs and short indels were detected using Freebayes 1.3.1 (Garrison & Marth, 2012), with a filter on the minimum fraction of observations supporting a variant (F = 0.03), disabling population priors (-k argument) and using an aggregate probability of observation balance between alleles (-a argument). Variants were then filtered using a custom R script. This script

selected only variable positions for which the read total depth was over 200 and for which the alternative allele was supported by at least 10 reads within a tissue (*Wolbachia* genome coverage - mean ± se: ovaries = 723.9 reads ± 134.8, nerve chain = 769.8 ± 81.0, haemolymph = 533.7).

2.7 Variant validation

As the *A. vulgare* lineage used in our experiments may contain nuclear inserts absent from the reference genome used for read mapping (Chebbi et al., 2019) the risk that sequences from *Wolbachia*-derived nuclear inserts generated spurious SNPs may not have been eliminated. To exclude remaining spurious SNPs, we implemented a three-step approach. (**1**) We checked that the sequences containing candidate SNPs were absent from uninfected individuals sequenced in previous studies, using all short-read data generated by (Chebbi et al., 2019) and (Cordaux et al., 2021). These data constitute whole genome sequences of six pools of 10 males or females and five individuals, from three uninfected lineages. We aligned these short reads with bwa-mem2 on the *w*VulC reference sequence. On the 11 resulting alignment files, variant calling was carried out with the same parameters as above, but only at positions of detected candidate *Wolbachia* variants. All variants for which the alternative allele was present in the reads sequenced from uninfected individuals were eliminated. We then defined a 300-bp window around the position of each remaining variant (starting 150 bp before the site) and excluded variants in windows containing at least two reads from uninfected individuals. (**2**) To further check that each remaining variable region was absent from uninfected individuals, we then designed PCR primers to amplify 120-250 bp targets encompassing the focal variant. These primers were tested on two females from the recipient lineage (i.e., uninfected by *Wolbachia*), on two females from the source line (i.e., infected by *Wolbachia*) and on two of their brothers (not infected by *Wolbachia,* since infection induces feminization). If the primers

amplified DNA from at least one non-infected host, then the variant was eliminated. (**3**) Finally, we checked whether sequencing reads carrying non-reference SNP alleles represented sequences that were exceedingly divergent from the reference strain (e.g., insertions of *Wolbachia* DNA into the host genome, or a related bacterium). To do so, we automatically analyzed every candidate SNP via a script that parses the alignment (.bam) files of reads generated in this experiment. This script records the proportion of clipped reads, the proportion of read pairs that were aligned in proper pairs and the number of mismatches between reads and the reference (excluding the SNP itself). The script then performs Fisher exact tests to evaluate if these proportions significantly differ between reads carrying the reference allele and reads carrying the alternativeallele. Any SNP for which the p-value of any test was below 5% (after false discovery rate correction) was excluded. Lastly, the sequencing depth around SNPs that had passed all filters was averaged over 100-bp windows, via samtools depth, and plotted to check for anomalies, mainly the presence of collapsed repeated regions not fully resolved in the *Wolbachia* reference genome assembly.

To predict the effect of retained SNPs and indels on proteins coded by annotated genes, we used SNPeff 5.2c (Cingolani et al., 2012). Functional domains in these proteins were annotated using the InterProScan online service (http://www.ebi.ac.uk/interpro/, database release 100.0, (Paysan-Lafosse et al., 2023)).

2.8 Screening for variants in maternal lines

To determine whether the *Wolbachia* variant(s) validated by our filtration procedure (see above) arose during the focal individuals' lifetime or were maternally inherited, we searched for these variants in their maternal lineage. Specifically, we extracted DNA from the ovaries of sisters and maternal ancestors of focal individuals, going back six generations thanks to our broodstock collection stored at -20°C. The variants as well as the *Wolbachia* reference lineage

were searched by amplification-refractory mutation system (ARMS, (C. R. Newton et al., 1989)). For this purpose, for each variant we designed a couple of primers targeting either the reference allele or the variant allele (see primers in appendix 1). ARMS analyses were performed in a 25 µl reaction volume containing 0.5 µl genomic DNA, 5 µl 5X buffer (Promega), 0.5 µl dNTP, 1.25 µl forward and reverse primers and 0.125 µl GoTaq® polymerase (Promega). The volume was adjusted to 25 µl with double-distilled water. PCR regimen was as follows: initial denaturation at 95°C for 5 min, followed by 35 cycles for 30 s at 95°C, 30 s at 61°C, 30 s at 72°C, and then a final extension for 5 min at 72°C, and finally the PCR products were maintained at 4°C in the end. PCR products were separated on a 1.5% agarose gel (23min., 100V).

2.9 Statistical Analyses

Statistical analyses were carried out using the R software (R Core Team, 2022). The influence of the tissular origin of the injected *Wolbachia* on *A. vulgare* mortality was evaluated using the 'survreg' function with either exponential or Weibull errors distribution ('survival' package, (Therneau et al., 2024)). The model included survival as a response variable, and infection status (i.e., injected with *Wolbachia*-infected or uninfected tissue filtrate), tissue origin of the injected filtrate and experimental block as explanatory variables. The influence of *Wolbachia* tissue origin on its ability to colonize and infect different focal tissues of recipient hosts over time was assessed using a generalized linear mixed model (GLMM). Log-transformed relative quantification (RQ) values representing the per-host cell *Wolbachia* dose were fitted as a response variable, assuming normal error distribution. The tissular origin of *Wolbachia*, the focal tissue of recipient injected hosts and the day post injection were used as explanatory variables. The quadratic term day post injection was added to assess whether it significantly improved the model fit. Individual IDs nested in experimental block were

specified as random-effect variables in the model. To compare *Wolbachia* loads measured in the tissues of recipient hosts six months after experimental infection with that measured in the same tissues from females of the same age but naturally infected by *Wolbachia* (from the WXw line), we ran, for each tissue, a linear model with log-transformed relative quantification (RQ) values fitted as a response variable and the origin of the individuals (i.e., naturally infected or experimentally infected) as an explanatory variable.

Maximal models including all higher-order interactions were simplified by sequentially eliminating non-significant terms and interactions to establish a minimal model (Crawley, 2012). The significance of the effects of explanatory variables was established using a likelihood ratio test (LRT, (Crawley, 2012)) whose statistics approximately follows a Chi-square distribution (Bolker, 2008) or an F test. The significant LRT or F value given in the Results section are for the minimal model, whereas non-significant values correspond to those obtained before the deletion of the variables from the model. *A posteriori* contrasts were carried out by aggregating factor levels together and by testing the fit of the simplified model using a likelihood-ratio test (Bolker, 2008; Crawley, 2012).

3. Results

3.1 *Wolbachia* infection does not significantly influence host survival

Under the assumption of both exponential errors and non-constant hazard, no effect of *Wolbachia* tissue origin on the survival rate of *A. vulgare* during early stage of infection (from day 0 to 60, trans-infection experiment 1) was detected (exponential errors: LRT = 0.600, p = 0.740, Weibull errors: LRT = 0.602, p = 0.741, **Fig. 1A**). Overall, the injection of *Wolbachia*, irrespective of its tissue origin, was not shown to influence the survival of individuals (exponential errors: LRT = 1.040, p = 0.308, Weibull errors: LRT = 1.039, p = 0.307). Sixty days

after injection, the survival rate of infected individuals was 0.87 (± 95% CI, ± 0.79-0.96), compared to 0.80 (± 0.71-0.91) for control animals.

In the trans-infection batches used to investigate the influence of *Wolbachia* tissue origin on its ability to persist in recipient host tissue (trans-infection experiment 2), the mortality of animals was also not significantly influenced by *Wolbachia* tissue origin (exponential errors: LRT = 2.65, p = 0.265, Weibull errors: LRT = 2.88, p = 0.236) or even just by the fact of being infected by the bacteria (whatever the origin of the tissue, exponential errors: LRT = 2.22, p = 0.136, Weibull errors: LRT = 2.45, p = 0.117, **Fig. 1B**). The survival rate of infected individuals 200 days after the experimental infection was 0.59 ± 0.48-0.74 and 0.47 ± 0.36-0.61 for infected and control animals respectively.

3.2 The tissue origin of *Wolbachia* influences its early infection dynamics in recipient host tissues (trans-infection experiment 1)

After injection, the presence of *Wolbachia* was detected by qPCR in the three tested tissues of all recipient hosts, confirming its ability to colonize a new host. *Wolbachia* density increased over time (post-injection day: LRT = 16.239, p < 0.0001) and fitting the quadratic term ($day\_post\_injection^2$) strongly improved model fit (LRT = 32.181, p < 0.0001), suggesting that *Wolbachia* burden was more accurately modelled by an accelerated polynomial function of day post-injection (**Fig. 2A**). The density of *Wolbachia* in tissues started very low on day 20 post-injection, then rose slightly between day 20 and day 40, to drastically increase between day 40 and day 60 post-injection. Although the pattern of infection in the different recipient tissues was overall similar, *Wolbachia* load was significantly influenced by the interaction between the colonized recipient tissue and the day post-injection (LRT = 74.309, p < 0.0001). The dynamics of infection within the nerve chain were significantly different from those

observed in the haemolymph and ovaries, leading to a higher bacterial load in nerve tissues 60 days post-infection (LRT = 57.228, $p < 0.0001$, LRT = 122.240, $p < 0.0001$, respectively, **Fig. 2A**). The dynamics of infection were also significantly different within haemolymph and ovaries (LRT = 17.771, p = 0.0013, **Fig. 2A**), as bacterial load was lower in ovaries at the end of monitoring (mean RQ ± se, nerve chain = 6.582 ± 1.596, haemolymph = 4.864 ± 1.612, ovaries = 2.533 ± 0.594, **Fig. 2A**). *Wolbachia* infection dynamics were also influenced by the tissue origin of the injected bacteria (interaction between days post-injection and tissue origin: LRT = 24.205, $p < 0.0001$). Whether the bacteria came from the haemolymph or ovaries of naturally infected animals did not significantly affect the colonization dynamics of *Wolbachia* in the injected recipients (LRT = 0.647, p = 0.723, **Fig. 2B**). However, bacteria from the nerve chain colonized recipient hosts less rapidly than bacteria from other tissues (nerve chain versus haemolymph: LRT = 28.981, $p < 0.0001$, nerve chain versus ovaries: LRT = 33.64, $p < 0.0001$). At 60 days post-injection, the *Wolbachia* load was on average more than twice as high when the bacteria came from the ovaries and haemolymph than when they came from the nerve chain of infected source hosts (mean RQ ± se, ovaries = 8.191 ± 2.18, haemolymph = 5.26 ± 1.077, nerve chain = 0.899 ± 0.197, **Fig. 2B**). However, there was no significant interaction between the colonized recipient tissue and the *Wolbachia's* original tissue, suggesting that bacteria originating from a tissue do not colonize that same tissue more effectively in recipient hosts (LRT = 6.957, p = 0.138).

3.3 The tissue origin of *Wolbachia* does not influence significantly its persistence in recipient host tissues (trans-infection experiment 2)

Wolbachia densities at 200 days after infection were significantly different between tissues from the recipient hosts (LRT = 39.224, $p < 0.0001$, **Fig. 3**). Bacterial load was the highest in

the nerve chain and the lowest in the haemolymph (contrast analyses, haemolymph versus nerve chain: LRT = 38.133, $p < 0.0001$, haemolymph versus ovaries: LRT = 20.823, $p < 0.0001$, nerve chain versus ovaries: LRT = 6.969, $p = 0.008$, **Fig. 3**). The bacterial load in the ovaries and haemolymph of recipient females were similar to those observed in the same tissues of females naturally infected by *Wolbachia* (source lineage, F = 0.184, $p = 0.672$, F = 0.268, $p = 0.609$, respectively, **Fig. 3 & 4**). In contrast, bacterial density in the nerve chain of experimentally infected females was on average more than twice that measured in the nerve chain of naturally infected individuals (F = 38.089, $p < 0.0001$, **Fig. 3 & 4**).

Contrary to what was observed during the early phase of infection, there was no effect of the tissue origin of *Wolbachia* on the bacterial load in recipient tissues at 200 days post-injection (LRT = 0.368, $p = 0.832$). Similarly, *Wolbachia* density in recipient tissues was not influenced by the interaction between the colonized tissue and the tissue origin of the injected bacteria (LRT = 9.539, $p = 0.059$).

3.4 Complete genome assembly of the *w*VulC *Wolbachia* strain

Using ONT reads, a complete circular genome sequence (1,638,144 bp) of the *w*VulC *Wolbachia* strain was assembled. The estimated completeness of the assembly was very high, with 99.8% of the expected BUSCO genes found in the sequence (C: 99.8% [S: 99.5%, D: 0.3%], F: 0.0%). The annotation of the genome resulted in 1,390 protein-coding sequences and 208 pseudogenes (**Fig. 5**). The *w*VulC genome contained 138 IS elements that are larger than 150 bp, representing 8.45% of the total length of the genome. This high proportion of repeated sequences for a bacterium is similar to that of other *Wolbachia* strains (Cerveau et al., 2011). We also identified seven prophage regions (six intact and one questionable region, following PHASTEST scoring criteria), representing 12.1% of the *w*VulC genome.

3.5 Whole-genome resequencing and variant calling reveal *Wolbachia* genome stability

The variant calling performed using the whole-genome resequencing of tissues from three females naturally infected by *Wolbachia* (i.e., source lineage) detected 641 SNPs and short indels. However, 584 of these apparent variants were also detected in the resequenced genome of several *A. vulgare* lineages not infected by *Wolbachia* (validation procedure, step 1), meaning that these variants probably amounted to *Wolbachia* sequences inserted into the host nuclear genome. The presence of reads sequenced from uninfected hosts within a 300-bp window around the 57 remaining polymorphic regions resulted in the exclusion of 26 variants (validation procedure step 2). Of the remaining 31 SNPs and small indels, 7 were excluded because their regions were PCR-amplified in males not infected with *Wolbachia* (infection status confirmed by qPCR, validation procedure step 3). Finally, in the last step of variant validation, we excluded 23 variants due to anomalies detected, such as a high proportion of clipped reads and/or a high number of mismatches between reads and reference. Overall, only 0.15% (one SNP) of the originally detected variants were finally validated. This unique SNP was observed in a single individual (F_1999). The frequency of this variant varied slightly among the three tissues (**Table 1**). The mutation affected a protein-coding gene, with a non-synonymous substitution (**Table 1**, **Fig. 5**). The putative protein did not have any recognized functional domain. The variant was not detected in the F_1999 individual's sisters, and was also absent from all females tested in the maternal line (traced back 6 generations, see appendix 1).

4. Discussion

Experimental trans-infections enabled us to study the influence of the tissue origin of *Wolbachia* on the early infection dynamics of the endosymbiont in different recipient host

tissues, and the ability of each bacterial sub-population to establish a chronic infection. At the same time, regular monitoring of injected individuals over a period of six months shed light on the influence of *Wolbachia* on the survival rate of recipient hosts and did not reveal any difference between *Wolbachia* sub-populations with respect to their virulence. In addition, our results corroborate a previous report showing a similar survival rate between trans-infected and un-infected animals (Le Clec'h et al., 2012). As the source and recipient lines belonged to the same field-collected *A. vulgare* population, they should be ecologically similar for *Wolbachia*. Low virulence is therefore expected, as for most vertically transmitted endosymbionts transferred between closely related hosts (Le Clec'h et al., 2013).

Colonization of recipient female tissues was relatively fast, with a threefold increase in *Wolbachia* density between the second and sixth month after infection. At the end of the experiment, the bacterial load in the tissues of the recipient females was similar to, or even higher than, that observed in the tissues of naturally vertically infected females.

Nevertheless, although rapid, the dynamics of *Wolbachia* infection varied according to the tissue origin of the bacteria. Bacteria from the nerve chain colonized recipient hosts much less rapidly than bacteria from ovaries and haemolymph. Two months after infection with a similar dose of bacteria, *Wolbachia* load was more than twice as low in hosts injected with bacteria from nerve chain, compared with hosts infected by bacteria from the other two tissues. The growth rate of bacteria is known to largely vary according to the type and amount of nutrients available in their environment (Keiblinger et al., 2010; Liu et al., 2005). The lower growth rate of bacteria from nerve chain, compared with those from the other tissues, could therefore be explained by the fact that in naturally infected hosts, this tissue is less favourable to the development of *Wolbachia* (e.g., poorer in resources). If so, bacteria from the nerve chain could be subject to growth-limiting stress at the time of their horizontal transfer, which

would explain their lower replication rate within the recipient host at the start of infection. However, the nerve chain was the recipient host tissue the most rapidly colonized by *Wolbachia* after trans-infection, and the one showing the highest bacterial load at each sampling point irrespective of the tissue origin of the bacteria. As well as showing no tropism towards the tissue of origin, this result suggests that nervous tissue is actually favourable to the development of *Wolbachia.*

Alternatively, the lower growth rate from bacteria originating from the nerve chain could be adaptive. Classic theory for the evolution of virulence is based on a trade-off between parasite growth, transmission and host survival, which predicts that higher growth increases not only transmission but also virulence (Alizon et al., 2009; Frank, 1996). *Wolbachia* transmission is essentially maternal (Turelli et al., 2018; Werren et al., 2008), but cases of non-maternal transmission have been observed *in natura* (Durand et al., 2024; Sanaei et al., 2021) and in the laboratory (Le Clec'h et al., 2013; Rigaud & Juchault, 1995). In a tissue not directly involved in parasite transmission, we predicted that virulence should constrain the parasite growth to low levels. Our results corroborate this prediction, as *Wolbachia* from the nerve chain of *A. vulgare* should not be transmissible – except maybe in rare cases of cannibalism and predation (Le Clec'h et al., 2013) – and may prove detrimental to the host if they proliferate. Uncontrolled colonization of nerve cells has indeed been shown to alter host behaviour in several *Wolbachia*-host pairs (Bi & Wang, 2020; Le Clec'h et al., 2012), and to lead to severe tissue degeneration and premature host death (Kosmidis et al., 2014; W. L. Le Clec'h et al., 2012; Min & Benzer, 1997; Strunov & Kiseleva, 2016). In tissues that allow parasite transmission, the balance between *Wolbachia* growth and host fitness should favour higher growth rates. In terrestrial isopods, both ovaries and haemolymph play a key role in both intra- and inter-host dissemination of *Wolbachia*. Ovaries are the route for vertical

transmission and haemolymph, in addition to participating in the dissemination of the bacteria across host tissues (Braquart-Varnier et al., 2015; Sanaei et al., 2021), may also be involved in horizontal transfer via contact between injured individuals (Rigaud & Juchault, 1995).

Although initial differences were observed at two months post-infection, the tissue origin of the injected *Wolbachia* had no significant effect on bacterial load in the three tissues analysed four months later (i.e., 6 months post-injection). The convergence of growth rates over time suggests that the early phenotypic variability observed two months post-infection may result from phenotypic plasticity. This interpretation is further supported by the absence of recurrent small genomic variations associated with tissue types in naturally infected individuals from the source lineage. More broadly, SNP and small indel analyses revealed a single substitution detected across sequence data from seven tissue samples. This SNP, observed in one female (F_1999), was nevertheless present in all three *Wolbachia* subpopulations, with allelic frequencies ranging from 24% to 58% depending on the tissue. This mutation, located in a gene coding for a protein of unknown function, leads to an amino acid substitution. Although we currently have no information on the phenotypic impact of this mutation, amino acid substitution may have strong phenotypic effects in bacteria (e.g., (Abdelaal et al., 2009; Bacigalupe et al., 2019)).

The variant, although predominant in the nerve chain, was present at lower frequencies in the ovaries. Nevertheless, over a quarter of the *Wolbachia* population in this tissue carried the mutation. This suggests that some of the female's oocytes may have been colonized by the variant and that, despite the suspicion of a strong bottleneck, it could have passed it on to its offspring (Chrostek & Teixeira, 2015). However, this hypothesis could not be verified in our study, as the female was sacrificed before reproducing. What is clear is that the absence of this SNP within the individual's maternal lineage strongly suggests that this

Wolbachia variant arose during its lifetime. The emergence of *Wolbachia* variants within just a few host generations or even during a host's lifetime has been documented (Chrostek & Teixeira, 2018; Martinez & Sinkins, 2023; Namias et al., 2024; Newton & Sheehan, 2015). However, most reported variants were associated with structural genomic changes rather than point genomic mutations (e.g., (Chrostek & Teixeira, 2018; Namias et al., 2024)). We currently have no information on the presence of structural genomic changes within the different *Wolbachia* tissular subpopulations, but in agreement with reports from other symbiotic systems, the very low number of point mutations observed in our study tends to support the stability of the *Wolbachia* genome (Dainty et al., 2021; Huang et al., 2020; Ross et al., 2022; Trouche et al., 2024).

In conclusion, our study reveals that within-host environmental heterogeneity can lead to diverse phenotypes in the most widespread bacterial endosymbiont in animals, *Wolbachia*. This variability did not appear to result from genomic variation, but from phenotypic plasticity. From a methodological point of view, we showed that the detection of variants in endosymbiont populations requires considerable caution, as our conservative approach led us to exclude more than 99.85% of the initially called variants. We recommend the use of a rigorous step-by-step approach to eliminate spurious genetic variants caused by the presence of endosymbiont genomic sequences inserted into the host genome.

Data accessibility statement

The R scripts and data supporting the conclusions of this article are available on the Figshare data repository (https://figshare.com/s/b1f84643b65b4f897c54). To ensure the stability and reliability of the command-lines used for genome assembly and SNP calling we have included all necessary information and options in the github repository (https://github.com/UMR-CNRS-7267/Wolbachia_endosymbiont_heterogeneity_paper). We have taken proactive

measures to address potential volatility on GitHub by uploading a compressed archive of this GitHub methodology to the Figshare data repository. Raw sequencing data have been deposited in GenBank (*w*VulC genome assembly: BioProject PRJNA1116085; *Wolbachia* resequencing: PRJNA1117639).

Author's contributions

R.P. and R.C. conceived and designed the experiments. R.P., R.J., M.P. and M.R. performed the trans-infection experiments. RP, TU, WA performed the preliminary experiment. RP and C.D prepared the samples for resequencing and C.D, TB and TU carried out the PCRs. D.O. performed *Wolbachia* genome sequencing. Y.D. assembled the *Wolbachia* genome. R.P., Y.D., B.M. and J.P. analysed the data. R.P. wrote the first draft of the manuscript, and all authors contributed substantially to revision.

Competing interests

We declare we have no competing interests.

Funding

This work was funded by Agence Nationale de la Recherche Grants ANR-21-CE02-0004 (RESIST) to RC and ANR-20-CE02-004 (SymChroSex) to JP, and intramural funds from the CNRS and the University of Poitiers.

Acknowledgements

We thank Isabelle Giraud for the extraction of the DNA used to sequence and assemble the genome of *Wolbachia w*VulC and Pierre Grève and Didier Bouchon for providing us with preliminary data so that we could fine-tune the bioinformatics analyses. We would like to thank Alexandra Lafitte for her invaluable work supervising the breeding of *A. vulgare*.

5. References

Abdelaal, A., El-Ghaffar, H. A., Zaghloul, M. H. E., El Mashad, N., Badran, E., & Fathy, A. (2009). Genotypic detection of rifampicin and isoniazid resistant *Mycobacterium tuberculosis* strains by DNA sequencing: A randomized trial. *Annals of Clinical Microbiology and Antimicrobials*, *8*(1), 4. https://doi.org/10.1186/1476-0711-8-4

Ailloud, F., Didelot, X., Woltemate, S., Pfaffinger, G., Overmann, J., Bader, R. C., Schulz, C., Malfertheiner, P., & Suerbaum, S. (2019). Within-host evolution of *Helicobacter pylori* shaped by niche-specific adaptation, intragastric migrations and selective sweeps. *Nature Communications*, *10*(1), Article 1. https://doi.org/10.1038/s41467-019-10050-1

Alizon, S., Hurford, A., Mideo, N., & Van Baalen, M. (2009). Virulence evolution and the trade-off hypothesis: History, current state of affairs and the future. *Journal of Evolutionary Biology*, *22*(2), 245–259. https://doi.org/10.1111/j.1420-9101.2008.01658.x

Avettand-Fenoel, V., Hocqueloux, L., Müller-Trutwin, M., Prazuck, T., Melard, A., Chaix, M.-L., Agoute, E., Michau, C., & Rouzioux, C. (2011). Greater diversity of HIV DNA variants in the rectum compared to variants in the blood in patients without HAART. *Journal of Medical Virology*, *83*(9), 1499–1507. https://doi.org/10.1002/jmv.22132

Bacigalupe, R., Tormo-Mas, M. Á., Penadés, J. R., & Fitzgerald, J. R. (2019). A multihost bacterial pathogen overcomes continuous population bottlenecks to adapt to new host species. *Science Advances*, *5*(11), eaax0063. https://doi.org/10.1126/sciadv.aax0063

614 Ben-Hur, E., & Kadmon, R. (2020). Heterogeneity–diversity relationships in sessile organisms:
615 A unified framework. *Ecology Letters*, *23*(1), 193–207.
616 https://doi.org/10.1111/ele.13418
617 Bessière, P., & Volmer, R. (2021). From one to many: The within-host rise of viral variants.
618 *PLOS Pathogens*, *17*(9), e1009811. https://doi.org/10.1371/journal.ppat.1009811
619 Bi, J., & Wang, Y. (2020). The effect of the endosymbiont *Wolbachia* on the behavior of
620 insect hosts. *Insect Science*, *27*(5), 846–858. https://doi.org/10.1111/1744-
621 7917.12731
622 Bolker, B. M. (2008). *Ecological Models and Data in R*. Princeton, Princeton University Press.
623 Braquart-Varnier, C., Raimond, M., Mappa, G., Chevalier, F. D., Le Clec'h, W., & Sicard, M.
624 (2015). The Hematopoietic organ: A cornerstone for *Wolbachia* propagation between
625 and within Hosts. *Frontiers in Microbiology*, *6*.
626 https://doi.org/10.3389/fmicb.2015.01424
627 Burnett, M. R., August, P. V., Brown, J. H., & Killingbeck, K. T. (1998). The influence of
628 geomorphological heterogeneity on biodiversity: I. A patch-scale perspective.
629 *Conservation Biology*, *12*(2), 363–370.
630 Cerveau, N., Leclercq, S., Leroy, E., Bouchon, D., & Cordaux, R. (2011). Short- and Long-term
631 evolutionary dynamics of bacterial insertion sequences: Insights from *Wolbachia*
632 endosymbionts. *Genome Biology and Evolution*, *3*, 1175–1186.
633 https://doi.org/10.1093/gbe/evr096
634 Chebbi, M. A., Becking, T., Moumen, B., Giraud, I., Gilbert, C., Peccoud, J., & Cordaux, R.
635 (2019). The Genome of *Armadillidium vulgare* (Crustacea, Isopoda) provides insights
636 into sex chromosome evolution in the context of cytoplasmic sex determination.

637 *Molecular Biology and Evolution*, *36*(4), 727–741.
638 https://doi.org/10.1093/molbev/msz010
639 Chen, S., Zhou, Y., Chen, Y., & Gu, J. (2018). fastp: An ultra-fast all-in-one FASTQ
640 preprocessor. *Bioinformatics*, *34*(17), i884–i890.
641 https://doi.org/10.1093/bioinformatics/bty560
642 Chrostek, E., & Teixeira, L. (2015). Mutualism breakdown by amplification of *Wolbachia*
643 genes. *PLOS Biology*, *13*(2), e1002065. https://doi.org/10.1371/journal.pbio.1002065
644 Chrostek, E., & Teixeira, L. (2018). Within host selection for faster replicating bacterial
645 symbionts. *PLoS ONE*, *13*(1). https://doi.org/10.1371/journal.pone.0191530
646 Cingolani, P., Platts, A., Wang, L. L., Coon, M., Nguyen, T., Wang, L., Land, S. J., Lu, X., &
647 Ruden, D. M. (2012). A program for annotating and predicting the effects of single
648 nucleotide polymorphisms, SnpEff: SNPs in the genome of *Drosophila melanogaster*
649 strain w1118; iso-2; iso-3. *Fly*, *6*(2), 80–92. https://doi.org/10.4161/fly.19695
650 Clement, S., Vaudaux, P., Francois, P., Schrenzel, J., Huggler, E., Kampf, S., Chaponnier, C.,
651 Lew, D., & Lacroix, J.-S. (2005). Evidence of an intracellular reservoir in the nasal
652 mucosa of patients with recurrent *Staphylococcus aureus* rhinosinusitis. *The Journal*
653 *of Infectious Diseases*, *192*(6), 1023–1028. https://doi.org/10.1086/432735
654 Cordaux, R., Chebbi, M. A., Giraud, I., Pleydell, D. R. J., & Peccoud, J. (2021). Characterization
655 of a sex-determining region and its genomic context via statistical estimates of
656 haplotype frequencies in daughters and sons sequenced in pools. *Genome Biology*
657 *and Evolution*, *13*(8), evab121. https://doi.org/10.1093/gbe/evab121
658 Cordaux, R., & Gilbert, C. (2017). Evolutionary significance of *Wolbachia*-to-animal horizontal
659 gene transfer: Female sex determination and the f element in the isopod
660 *Armadillidium vulgare*. *Genes*, *8*(7), 186. https://doi.org/10.3390/genes8070186

661 Cordaux, R., Michel-Salzat, A., Frelon-Raimond, M., Rigaud, T., & Bouchon, D. (2004).
662 Evidence for a new feminizing *Wolbachia* strain in the isopod *Armadillidium vulgare*:
663 evolutionary implications. *Heredity*, *93*(1), 78–84.
664 https://doi.org/10.1038/sj.hdy.6800482
665 Crawley, M. J. (2012). *The R Book*. John Wiley & Sons.
666 Dainty, K. R., Hawkey, J., Judd, L. M., Pacidônio, E. C., Duyvestyn, J. M., Gonçalves, D. S., Lin,
667 S. Y., O'Donnell, T. B., O'Neill, S. L., Simmons, C. P., Holt, K. E., & Flores, H. A. (2021).
668 wMel *Wolbachia* genome remains stable after 7 years in Australian *Aedes aegypti*
669 field populations. *Microbial Genomics*, *7*(9), 000641.
670 https://doi.org/10.1099/mgen.0.000641
671 Danecek, P., Bonfield, J. K., Liddle, J., Marshall, J., Ohan, V., Pollard, M. O., Whitwham, A.,
672 Keane, T., McCarthy, S. A., Davies, R. M., & Li, H. (2021). Twelve years of SAMtools
673 and BCFtools. *GigaScience*, *10*(2), giab008.
674 https://doi.org/10.1093/gigascience/giab008
675 De Coster, W., D'Hert, S., Schultz, D. T., Cruts, M., & Van Broeckhoven, C. (2018). NanoPack:
676 Visualizing and processing long-read sequencing data. *Bioinformatics (Oxford,*
677 *England)*, *34*(15), 2666–2669. https://doi.org/10.1093/bioinformatics/bty149
678 Depeux, C., Branger, A., Paulhac, H., Pigeault, R., & Beltran-Bech, S. (2024). Deleterious
679 effects of *Wolbachia* on life history and physiological traits of common pill woodlice.
680 *Journal of Invertebrate Pathology*, *207*, 108187.
681 https://doi.org/10.1016/j.jip.2024.108187
682 Didelot, X., Walker, A. S., Peto, T. E., Crook, D. W., & Wilson, D. J. (2016). Within-host
683 evolution of bacterial pathogens. *Nature Reviews. Microbiology*, *14*(3), 150–162.
684 https://doi.org/10.1038/nrmicro.2015.13

685 Durand, S., Lheraud, B., Giraud, I., Bech, N., Grandjean, F., Rigaud, T., Peccoud, J., & Cordaux,
686 R. (2023). Heterogeneous distribution of sex ratio distorters in natural populations of
687 the isopod *Armadillidium vulgare*. *Biology Letters*, *19*(1), 20220457.
688 https://doi.org/10.1098/rsbl.2022.0457
689 Durand, S., Pigeault, R., Giraud, I., Loisier, A., Bech, N., Grandjean, F., Rigaud, T., Peccoud, J.,
690 & Cordaux, R. (2024). Temporal stability of sex ratio distorter prevalence in natural
691 populations of the isopod *Armadillidium vulgare*. *Heredity*, 1–11.
692 https://doi.org/10.1038/s41437-024-00713-1
693 Frank, S. A. (1996). Models of parasite virulence. *The Quarterly Review of Biology*, *71*(1), 37–
694 78. https://doi.org/10.1086/419267
695 Garrison, E., & Marth, G. (2012). *Haplotype-based variant detection from short-read*
696 *sequencing* (No. arXiv:1207.3907). arXiv. https://doi.org/10.48550/arXiv.1207.3907
697 Gupta, K., Toelzer, C., Williamson, M. K., Shoemark, D. K., Oliveira, A. S. F., Matthews, D. A.,
698 Almuqrin, A., Staufer, O., Yadav, S. K. N., Borucu, U., Garzoni, F., Fitzgerald, D., Spatz,
699 J., Mulholland, A. J., Davidson, A. D., Schaffitzel, C., & Berger, I. (2022). Structural
700 insights in cell-type specific evolution of intra-host diversity by SARS-CoV-2. *Nature*
701 *Communications*, *13*(1), Article 1. https://doi.org/10.1038/s41467-021-27881-6
702 Haft, D. H., Badretdin, A., Coulouris, G., DiCuccio, M., Durkin, A. S., Jovenitti, E., Li, W.,
703 Mersha, M., O'Neill, K. R., Virothaisakun, J., & Thibaud-Nissen, F. (2024). RefSeq and
704 the prokaryotic genome annotation pipeline in the age of metagenomes. *Nucleic*
705 *Acids Research*, *52*(D1), D762–D769. https://doi.org/10.1093/nar/gkad988
706 Houle, C., Pelletier, F., Bélisle, M., & Garant, D. (2020). Impacts of environmental
707 heterogeneity on natural selection in a wild bird population. *Evolution*, *74*(6), 1142–
708 1154. https://doi.org/10.1111/evo.13939

709 Huang, B., Yang, Q., Hoffmann, A. A., Ritchie, S. A., Hurk, A. F. van den, & Warrilow, D.
710 (2020). *Wolbachia* genome stability and mtDNA variants in *Aedes aegypti* field
711 populations eight years after release. *iScience*, *23*(10).
712 https://doi.org/10.1016/j.isci.2020.101572
713 Huang, B.-H., Huang, C.-W., Huang, C.-L., & Liao, P.-C. (2017). Continuation of the genetic
714 divergence of ecological speciation by spatial environmental heterogeneity in island
715 endemic plants. *Scientific Reports*, *7*(1), 5465. https://doi.org/10.1038/s41598-017-
716 05900-1
717 Huang, Y., Tran, I., & Agrawal, A. F. (2016). Does genetic variation maintained by
718 environmental heterogeneity facilitate adaptation to novel selection? *The American*
719 *Naturalist*, *188*(1), 27–37. https://doi.org/10.1086/686889
720 Hunt, M., Silva, N. D., Otto, T. D., Parkhill, J., Keane, J. A., & Harris, S. R. (2015). Circlator:
721 automated circularization of genome assemblies using long sequencing reads.
722 *Genome Biology*, *16*(1), 294. https://doi.org/10.1186/s13059-015-0849-0
723 Ioannidis, P., Hotopp, J. C. D., Sapountzis, P., Siozios, S., Tsiamis, G., Bordenstein, S. R., Baldo,
724 L., Werren, J. H., & Bourtzis, K. (2007). New criteria for selecting the origin of DNA
725 replication in *Wolbachia* and closely related bacteria. *BMC Genomics*, *8*(1), 182.
726 https://doi.org/10.1186/1471-2164-8-182
727 Johnson, P. T. J., Wood, C. L., Joseph, M. B., Preston, D. L., Haas, S. E., & Springer, Y. P.
728 (2016). Habitat heterogeneity drives the host-diversity-begets-parasite-diversity
729 relationship: Evidence from experimental and field studies. *Ecology Letters*, *19*(7),
730 752–761. https://doi.org/10.1111/ele.12609
731 Jorth, P., Staudinger, B. J., Wu, X., Hisert, K. B., Hayden, H., Garudathri, J., Harding, C. L.,
732 Radey, M. C., Rezayat, A., Bautista, G., Berrington, W. R., Goddard, A. F., Zheng, C.,

733 Angermeyer, A., Brittnacher, M. J., Kitzman, J., Shendure, J., Fligner, C. L., Mittler, J.,
734 … Singh, P. K. (2015). Regional isolation drives bacterial diversification within cystic
735 fibrosis lungs. *Cell Host & Microbe*, *18*(3), 307–319.
736 https://doi.org/10.1016/j.chom.2015.07.006
737 Jridi, C., Martin, J.-F., Marie-Jeanne, V., Labonne, G., & Blanc, S. (2006). Distinct Viral
738 Populations differentiate and evolve independently in a single perennial host plant.
739 *Journal of Virology*, *80*(5), 2349–2357. https://doi.org/10.1128/jvi.80.5.2349-
740 2357.2006
741 Kamiya, T., O'Dwyer, K., Nakagawa, S., & Poulin, R. (2014). Host diversity drives parasite
742 diversity: Meta-analytical insights into patterns and causal mechanisms. *Ecography*,
743 *37*(7), 689–697.
744 Kaur, R., Shropshire, J. D., Cross, K. L., Leigh, B., Mansueto, A. J., Stewart, V., Bordenstein, S.
745 R., & Bordenstein, S. R. (2021). Living in the endosymbiotic world of *Wolbachia*: A
746 centennial review. *Cell Host & Microbe*, *29*(6), 879–893.
747 https://doi.org/10.1016/j.chom.2021.03.006
748 Keiblinger, K. M., Hall, E. K., Wanek, W., Szukics, U., Hämmerle, I., Ellersdorfer, G., Böck, S.,
749 Strauss, J., Sterflinger, K., Richter, A., & Zechmeister-Boltenstern, S. (2010). The effect
750 of resource quantity and resource stoichiometry on microbial carbon-use-efficiency.
751 *FEMS Microbiology Ecology*, *73*(3), 430–440. https://doi.org/10.1111/j.1574-
752 6941.2010.00912.x
753 Kolmogorov, M., Yuan, J., Lin, Y., & Pevzner, P. A. (2019). Assembly of long, error-prone
754 reads using repeat graphs. *Nature Biotechnology*, *37*(5), 540–546.
755 https://doi.org/10.1038/s41587-019-0072-8

Kosmidis, S., Missirlis, F., Botella, J. A., Schneuwly, S., Rouault, T. A., & Skoulakis, E. M. C. (2014). Behavioral decline and premature lethality upon pan-neuronal ferritin overexpression in *Drosophila* infected with a virulent form of *Wolbachia*. *Frontiers in Pharmacology*, *5*, 66. https://doi.org/10.3389/fphar.2014.00066

Krzywinski, M., Schein, J., Birol, I., Connors, J., Gascoyne, R., Horsman, D., Jones, S. J., & Marra, M. A. (2009). Circos: An information aesthetic for comparative genomics. *Genome Research*, *19*(9), 1639–1645. https://doi.org/10.1101/gr.092759.109

Langenheder, S., & Lindström, E. S. (2019). Factors influencing aquatic and terrestrial bacterial community assembly. *Environmental Microbiology Reports*, *11*(3), 306–315. https://doi.org/10.1111/1758-2229.12731

Le Clec'h, W. L., Braquart-Varnier, C., Raimond, M., Ferdy, J.-B., Bouchon, D., & Sicard, M. (2012). High Virulence of *Wolbachia* after host switching: When autophagy hurts. *PLOS Pathogens*, *8*(8), e1002844. https://doi.org/10.1371/journal.ppat.1002844

Le Clec'h, W. L., Chevalier, F. D., Genty, L., Bertaux, J., Bouchon, D., & Sicard, M. (2013). Cannibalism and predation as paths for horizontal passage of *Wolbachia* between terrestrial isopods. *PLOS ONE*, *8*(4), e60232. https://doi.org/10.1371/journal.pone.0060232

Le Clec'h, W., Raimond, M., Guillot, S., Bouchon, D., & Sicard, M. (2013). Horizontal transfers of feminizing versus non-feminizing *Wolbachia* strains: From harmless passengers to pathogens. *Environmental Microbiology*, *15*(11), 2922–2936. https://doi.org/10.1111/1462-2920.12172

Leclercq, S., Thézé, J., Chebbi, M. A., Giraud, I., Moumen, B., Ernenwein, L., Grève, P., Gilbert, C., & Cordaux, R. (2016). Birth of a W sex chromosome by horizontal transfer of

779 *Wolbachia* bacterial symbiont genome. *Proceedings of the National Academy of*
780 *Sciences*, *113*(52), 15036–15041. https://doi.org/10.1073/pnas.1608979113
781 LePage, D., & Bordenstein, S. R. (2013). *Wolbachia*: Can we save lives with a great pandemic?
782 *Trends in Parasitology*, *29*(8), 385–393. https://doi.org/10.1016/j.pt.2013.06.003
783 Li, W., O'Neill, K. R., Haft, D. H., DiCuccio, M., Chetvernin, V., Badretdin, A., Coulouris, G.,
784 Chitsaz, F., Derbyshire, M. K., Durkin, A. S., Gonzales, N. R., Gwadz, M., Lanczycki, C.
785 J., Song, J. S., Thanki, N., Wang, J., Yamashita, R. A., Yang, M., Zheng, C., … Thibaud-
786 Nissen, F. (2021). RefSeq: Expanding the prokaryotic genome annotation pipeline
787 reach with protein family model curation. *Nucleic Acids Research*, *49*(D1), D1020–
788 D1028. https://doi.org/10.1093/nar/gkaa1105
789 Lieberman, T. D., Wilson, D., Misra, R., Xiong, L. L., Moodley, P., Cohen, T., & Kishony, R.
790 (2016). Genomic diversity in autopsy samples reveals within-host dissemination of
791 HIV-associated *Mycobacterium tuberculosis*. *Nature Medicine*, *22*(12), Article 12.
792 https://doi.org/10.1038/nm.4205
793 Liu, M., Durfee, T., Cabrera, J. E., Zhao, K., Jin, D. J., & Blattner, F. R. (2005). Global
794 transcriptional programs reveal a carbon source foraging strategy by *Escherichia coli.*
795 *The Journal of Biological Chemistry*, *280*(16), 15921–15927.
796 https://doi.org/10.1074/jbc.M414050200
797 Manni, M., Berkeley, M. R., Seppey, M., & Zdobnov, E. M. (2021). BUSCO: Assessing genomic
798 data quality and beyond. *Current Protocols*, *1*(12), e323.
799 https://doi.org/10.1002/cpz1.323
800 Marçais, G., Delcher, A. L., Phillippy, A. M., Coston, R., Salzberg, S. L., & Zimin, A. (2018).
801 MUMmer4: A fast and versatile genome alignment system. *PLOS Computational*
802 *Biology*, *14*(1), e1005944. https://doi.org/10.1371/journal.pcbi.1005944

803 Martinez, J., & Sinkins, S. P. (2023). *Rapid evolution of* Wolbachia *genomes in mosquito cell*
804 *culture*. Evolutionary Biology. https://doi.org/10.1101/2023.09.20.558649
805 Mcdonald, J. F., & Ayala, F. J. (1974). Genetic response to environmental heterogeneity.
806 *Nature*, *250*(5467), 572–574. https://doi.org/10.1038/250572a0
807 Min, K. T., & Benzer, S. (1997). *Wolbachia*, normally a symbiont of *Drosophila*, can be
808 virulent, causing degeneration and early death. *Proceedings of the National Academy*
809 *of Sciences of the United States of America*, *94*(20), 10792–10796.
810 https://doi.org/10.1073/pnas.94.20.10792
811 Namias, A., Ngaku, A., Makoundou, P., Unal, S., Sicard, M., & Weill, M. (2024). Intra-lineage
812 microevolution of *Wolbachia* leads to the emergence of new cytoplasmic
813 incompatibility patterns. *PLOS Biology*, *22*(2), e3002493.
814 https://doi.org/10.1371/journal.pbio.3002493
815 Newton, C. R., Graham, A., Heptinstall, L. E., Powell, S. J., Summers, C., Kalsheker, N., Smith,
816 J. C., & Markham, A. F. (1989). Analysis of any point mutation in DNA. The
817 amplification refractory mutation system (ARMS). *Nucleic Acids Research*, *17*(7),
818 2503–2516. https://doi.org/10.1093/nar/17.7.2503
819 Newton, I. L. G., & Sheehan, K. B. (2015). Passage of *Wolbachia pipientis* through mutant
820 *Drosophila melanogaster* induces phenotypic and genomic changes. *Applied and*
821 *Environmental Microbiology*, *81*(3), 1032–1037. https://doi.org/10.1128/AEM.02987-
822 14
823 Obaldia, N., Meibalan, E., Sa, J. M., Ma, S., Clark, M. A., Mejia, P., Moraes Barros, R. R.,
824 Otero, W., Ferreira, M. U., Mitchell, J. R., Milner, D. A., Huttenhower, C., Wirth, D. F.,
825 Duraisingh, M. T., Wellems, T. E., & Marti, M. (2018). Bone marrow is a major

parasite reservoir in *Plasmodium vivax* infection. *mBio*, *9*(3). https://doi.org/10.1128/mBio.00625-18

Paysan-Lafosse, T., Blum, M., Chuguransky, S., Grego, T., Pinto, B. L., Salazar, G. A., Bileschi, M. L., Bork, P., Bridge, A., Colwell, L., Gough, J., Haft, D. H., Letunić, I., Marchler-Bauer, A., Mi, H., Natale, D. A., Orengo, C. A., Pandurangan, A. P., Rivoire, C., … Bateman, A. (2023). InterPro in 2022. *Nucleic Acids Research*, *51*(D1), D418–D427. https://doi.org/10.1093/nar/gkac993

Peccoud, J., Chebbi, M. A., Cormier, A., Moumen, B., Gilbert, C., Marcadé, I., Chandler, C., & Cordaux, R. (2017). Untangling heteroplasmy, structure, and evolution of an atypical mitochondrial genome by PacBio sequencing. *Genetics*, *207*(1), 269–280. https://doi.org/10.1534/genetics.117.203380

Pedersen, B. S., & Quinlan, A. R. (2018). Mosdepth: Quick coverage calculation for genomes and exomes. *Bioinformatics*, *34*(5), 867–868. https://doi.org/10.1093/bioinformatics/btx699

Pietri, J. E., DeBruhl, H., & Sullivan, W. (2016). The rich somatic life of *Wolbachia*. *MicrobiologyOpen*, *5*(6), 923–936. https://doi.org/10.1002/mbo3.390

Puterová, J., & Martínek, T. (2021). digIS: Towards detecting distant and putative novel insertion sequence elements in prokaryotic genomes. *BMC Bioinformatics*, *22*(1), 258. https://doi.org/10.1186/s12859-021-04177-6

Qian, H., Qian, S., Zhang, J., & Kessler, M. (2024). Effects of climate and environmental heterogeneity on the phylogenetic structure of regional angiosperm floras worldwide. *Nature Communications*, *15*(1), 1079. https://doi.org/10.1038/s41467-024-45155-9

R Core Team. (2022). *R: A language and environment for statistical computing.* [Computer software]. https://www.R-project.org/

Rainey, P. B., & Travisano, M. (1998). Adaptive radiation in a heterogeneous environment. *Nature*, *394*(6688), Article 6688. https://doi.org/10.1038/27900

Regoes, R. R., Nowak, M. A., & Bonhoeffer, S. (2000). Evolution of virulence in a heterogeneous host population. *Evolution*, *54*(1), 64–71. https://doi.org/10.1111/j.0014-3820.2000.tb00008.x

Rigaud, T., & Juchault, P. (1995). Success and failure of horizontal transfers of feminizing *Wolbachia* endosymbionts in woodlice. *Journal of Evolutionary Biology*, *8*(2), 249–255. https://doi.org/10.1046/j.1420-9101.1995.8020249.x

Robinson, J. T., Thorvaldsdóttir, H., Wenger, A. M., Zehir, A., & Mesirov, J. P. (2017). Variant review with the integrative genomics viewer. *Cancer Research*, *77*(21), e31–e34. https://doi.org/10.1158/0008-5472.CAN-17-0337

Ross, P. A., Robinson, K. L., Yang, Q., Callahan, A. G., Schmidt, T. L., Axford, J. K., Coquilleau, M. P., Staunton, K. M., Townsend, M., Ritchie, S. A., Lau, M.-J., Gu, X., & Hoffmann, A. A. (2022). A decade of stability for wMel *Wolbachia* in natural *Aedes aegypti* populations. *PLOS Pathogens*, *18*(2), e1010256. https://doi.org/10.1371/journal.ppat.1010256

Sanaei, E., Charlat, S., & Engelstädter, J. (2021). *Wolbachia* host shifts: Routes, mechanisms, constraints and evolutionary consequences. *Biological Reviews*, *96*(2), 433–453. https://doi.org/10.1111/brv.12663

Sicard, M., Chevalier, F., De Vlechouver, M., Bouchon, D., Grève, P., & Braquart-Varnier, C. (2010). Variations of immune parameters in terrestrial isopods: A matter of gender,

aging and *Wolbachia*. *Naturwissenschaften*, *97*(9), 819–826. https://doi.org/10.1007/s00114-010-0699-2

Sicard, M., Dittmer, J., Grève, P., Bouchon, D., & Braquart-Varnier, C. (2014). A host as an ecosystem: *Wolbachia* coping with environmental constraints. *Environmental Microbiology*, *16*(12), 3583–3607. https://doi.org/10.1111/1462-2920.12573

Stein, A., Gerstner, K., & Kreft, H. (2014). Environmental heterogeneity as a universal driver of species richness across taxa, biomes and spatial scales. *Ecology Letters*, *17*(7), 866–880. https://doi.org/10.1111/ele.12277

Stein, A., & Kreft, H. (2015). Terminology and quantification of environmental heterogeneity in species-richness research. *Biological Reviews of the Cambridge Philosophical Society*, *90*(3), 815–836. https://doi.org/10.1111/brv.12135

Strunov, A., & Kiseleva, E. (2016). *Drosophila melanogaster* brain invasion: Pathogenic *Wolbachia* in central nervous system of the fly. *Insect Science*, *23*(2), 253–264. https://doi.org/10.1111/1744-7917.12187

Tatusova, T., DiCuccio, M., Badretdin, A., Chetvernin, V., Nawrocki, E. P., Zaslavsky, L., Lomsadze, A., Pruitt, K. D., Borodovsky, M., & Ostell, J. (2016). NCBI prokaryotic genome annotation pipeline. *Nucleic Acids Research*, *44*(14), 6614–6624. https://doi.org/10.1093/nar/gkw569

Templé, N., & Richard, F.-J. (2015). Intra-cellular bacterial infections affect learning and memory capacities of an invertebrate. *Frontiers in Zoology*, *12*(1), 36. https://doi.org/10.1186/s12983-015-0129-6

Therneau, T. M., until 2009), T. L. (original S.->R port and R. maintainer, Elizabeth, A., & Cynthia, C. (2024). *survival: Survival Analysis* (Version 3.6-4) [Computer software]. https://cran.r-project.org/web/packages/survival/index.html

Trevail, A. M., Green, J. A., Bolton, M., Daunt, F., Harris, S. M., Miller, P. I., Newton, S., Owen, E., Polton, J. A., Robertson, G., Sharples, J., & Patrick, S. C. (2021). Environmental heterogeneity promotes individual specialisation in habitat selection in a widely distributed seabird. *Journal of Animal Ecology*, *90*(12), 2875–2887. https://doi.org/10.1111/1365-2656.13588

Trouche, B., Schrieke, H., Duron, O., Eren, A. M., & Reveillaud, J. (2024). *Wolbachia* populations across organs of individual *Culex pipiens*: Highly conserved intra-individual core pangenome with inter-individual polymorphisms. *ISME Communications*, ycae078. https://doi.org/10.1093/ismeco/ycae078

Turelli, M., Cooper, B. S., Richardson, K. M., Ginsberg, P. S., Peckenpaugh, B., Antelope, C. X., Kim, K. J., May, M. R., Abrieux, A., Wilson, D. A., Bronski, M. J., Moore, B. R., Gao, J.-J., Eisen, M. B., Chiu, J. C., Conner, W. R., & Hoffmann, A. A. (2018). Rapid global spread of wRi-like *Wolbachia* across multiple *Drosophila*. *Current Biology*, *28*(6), 963-971.e8. https://doi.org/10.1016/j.cub.2018.02.015

van Houte, S., Padfield, D., Gómez, P., Luján, A. M., Brockhurst, M. A., Paterson, S., & Buckling, A. (2021). Compost spatial heterogeneity promotes evolutionary diversification of a bacterium. *Journal of Evolutionary Biology*, *34*(2), 246–255. https://doi.org/10.1111/jeb.13722

Vasimuddin, Md., Misra, S., Li, H., & Aluru, S. (2019). Efficient architecture-aware acceleration of BWA-MEM for multicore systems. *2019 IEEE International Parallel and Distributed Processing Symposium (IPDPS)*, 314–324. https://doi.org/10.1109/IPDPS.2019.00041

Wernegreen, J. J., & Wheeler, D. E. (2009). Remaining flexible in old alliances: Functional plasticity in constrained mutualisms. *DNA and Cell Biology*, *28*(8), 371–382. https://doi.org/10.1089/dna.2009.0872

Werren, J. H., Baldo, L., & Clark, M. E. (2008). *Wolbachia*: Master manipulators of invertebrate biology. *Nature Reviews Microbiology*, *6*(10), 741–751. https://doi.org/10.1038/nrmicro1969

White, P. S., Choi, A., Pandey, R., Menezes, A., Penley, M., Gibson, A. K., de Roode, J., & Morran, L. (2020). Host heterogeneity mitigates virulence evolution. *Biology Letters*, *16*(1), 20190744. https://doi.org/10.1098/rsbl.2019.0744

Wick, R. R., & Holt, K. E. (2022). Polypolish: Short-read polishing of long-read bacterial genome assemblies. *PLOS Computational Biology*, *18*(1), e1009802. https://doi.org/10.1371/journal.pcbi.1009802

Wishart, D. S., Han, S., Saha, S., Oler, E., Peters, H., Grant, J. R., Stothard, P., & Gautam, V. (2023). PHASTEST: Faster than PHASTER, better than PHAST. *Nucleic Acids Research*, *51*(W1), W443–W450. https://doi.org/10.1093/nar/gkad382

Xiao, Y., Dolan, P. T., Goldstein, E. F., Li, M., Farkov, M., Brodsky, L., & Andino, R. (2017). Poliovirus intrahost evolution is required to overcome tissue-specific innate immune responses. *Nature Communications*, *8*(1), Article 1. https://doi.org/10.1038/s41467-017-00354-5

Yang, Z., Liu, X., Zhou, M., Ai, D., Wang, G., Wang, Y., Chu, C., & Lundholm, J. T. (2015). The effect of environmental heterogeneity on species richness depends on community position along the environmental gradient. *Scientific Reports*, *5*(1), 15723. https://doi.org/10.1038/srep15723

Table 1. Nucleotide difference between *Wolbachia* from three tissues of naturally infected *Armadillidium vulgare*. HAEM: haemolymph, NC: nerve chain, OVA: ovaries. Nucl: Nucleotide, AA: amino acid; Arg: arginine, Gln: glutamine

Genome position	Individual	Tissue	Frequency	Type of change	Nucl. change	AA change	ORF effect	Gene name	Functional domains
1269492	F1_2015	NC	0	Substitution	C -> T	Arg340Gln	Missense variant	ABOJ95_001275	No recognized functional domain
		OVA	0						
	F2_2015	NC	0						
		OVA	0						
	F_1999	HAEM	0.466						
		NC	0.584						
		OVA	0.239						

Figure captions

Figure 1. Survival rate of *Armadillidium vulgare* following *Wolbachia* (*w*VulC) trans-infection. Effect of tissue origin of injected *Wolbachia* on mortality of recipient hosts monitored (**A**) every 10 days from day 0 to day 60 post-injection and (**B**) every 15-20 days from day 0 to day 200 post-injection. Solid lines: recipient hosts injected with crushed filtered tissue from animals naturally infected by *Wolbachia w*Vulc. Dotted lines: control individuals injected with crushed filtered tissue *from A. vulgare* not infected by *Wolbachia.* The three colours correspond to the tissue of origin of Wolbachia. Green: nerve chain, red: ovaries, blue: haemolymph

Figure 2. Infection dynamics of *Wolbachia* (*w*VulC) in *Armadillidium vulgare* from day 0 to day 60 post-injection. (**A**) *Wolbachia* loads in nerve chain (green), haemolymph (blue) and ovaries (red) of recipient hosts trans-infected by *Wolbachia*, all source tissue considered. (**B**) Influence of *Wolbachia* tissue origin on infection dynamics in tissue loads in recipient host, all recipient tissue considered. Green: nerve chain, red: ovaries, blue: haemolymph. Error bars correspond to the standard error. Infection dynamics not connected by the same letter are significantly different ($p < 0.05$).

Figure 3. *Wolbachia* (*w*VulC) load in *Armadillidium vulgare* tissues six months post-injection. The coloured boxplots illustrate the tissue origin of Wolbachia (green: nerve chain, red: ovaries, blue: haemolymph). However, the analysis did not reveal any significant effect of the tissue origin of the bacteria on the intensity of infection (RQ) in the recipient host tissues. Boxes above and below the medians (horizontal lines) show the first and third quartiles, respectively. Black diamonds represent the means. Levels not connected by the same letter are significantly different ($p < 0.05$).

Figure 4 *Wolbachia* (*w*VulC) load in tissues from naturally infected females (source line). *Wolbachia* load was measured in the haemolymph, nerve chain and ovaries of 15 females from the source line. The analysis showed that the bacterial load was lower in the haemolymph than in the ovaries and nerve chain. Boxes above and below the medians (horizontal lines) show the first and third quartiles, respectively. Black diamonds represent the means. Levels not connected by the same letter are significantly different ($p < 0.05$). Green: nerve chain, red: ovaries, blue: haemolymph.

Figure 5. Circos plot of the *w*VulC *Wolbachia* genome. Prophage-derived regions are indicated inside the genome ideogram (outer track), with their colour corresponding to the score attributed by PHASTEST (dark blue: intact, light blue: questionable). Ticks on the ideogram are separated by 10 kb intervals, and indicated values are in Mb. Predicted protein-coding genes are represented by grey rectangles (second track), and Insertion Sequence elements by black rectangles (third track). In the fourth track, the normalized read coverage for 5 kb adjacent windows (averaged over recipient individuals) is represented for the different resequenced tissues: ovaries (red), nerve chain (green) and haemolymph (blue). The black line corresponds to a mean normalized coverage of one, and grey lines are separated by 0.1 unit. Black triangle indicates the position of the detected variant and the bold letter (C and T) correspond to the two alleles.

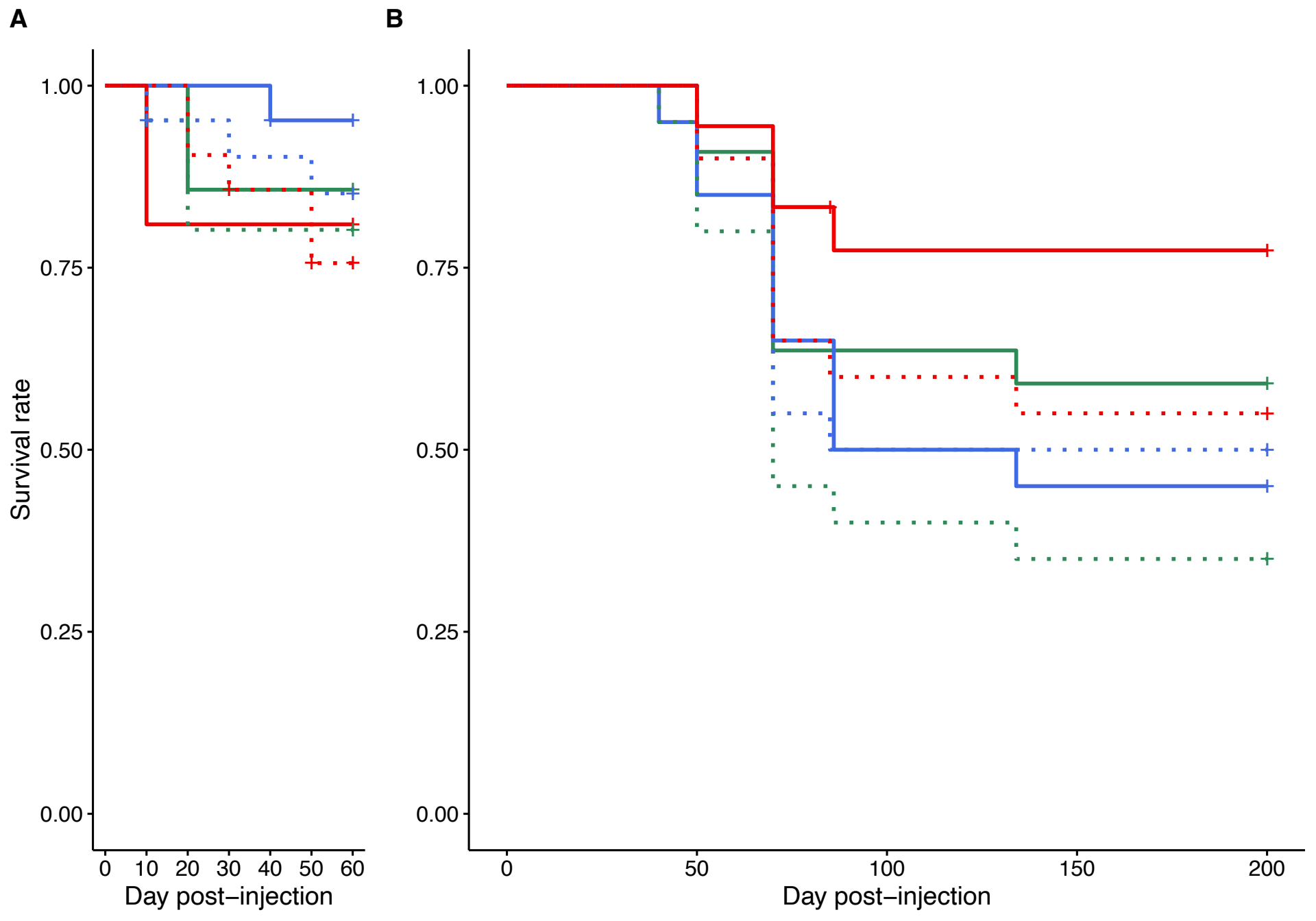
A
B
1.00
0.75
0.50
0.25
0.00
Survival rate
0
10
20
30
40
50
60
Day post−injection
0
50
100
150
200
Day post−injection

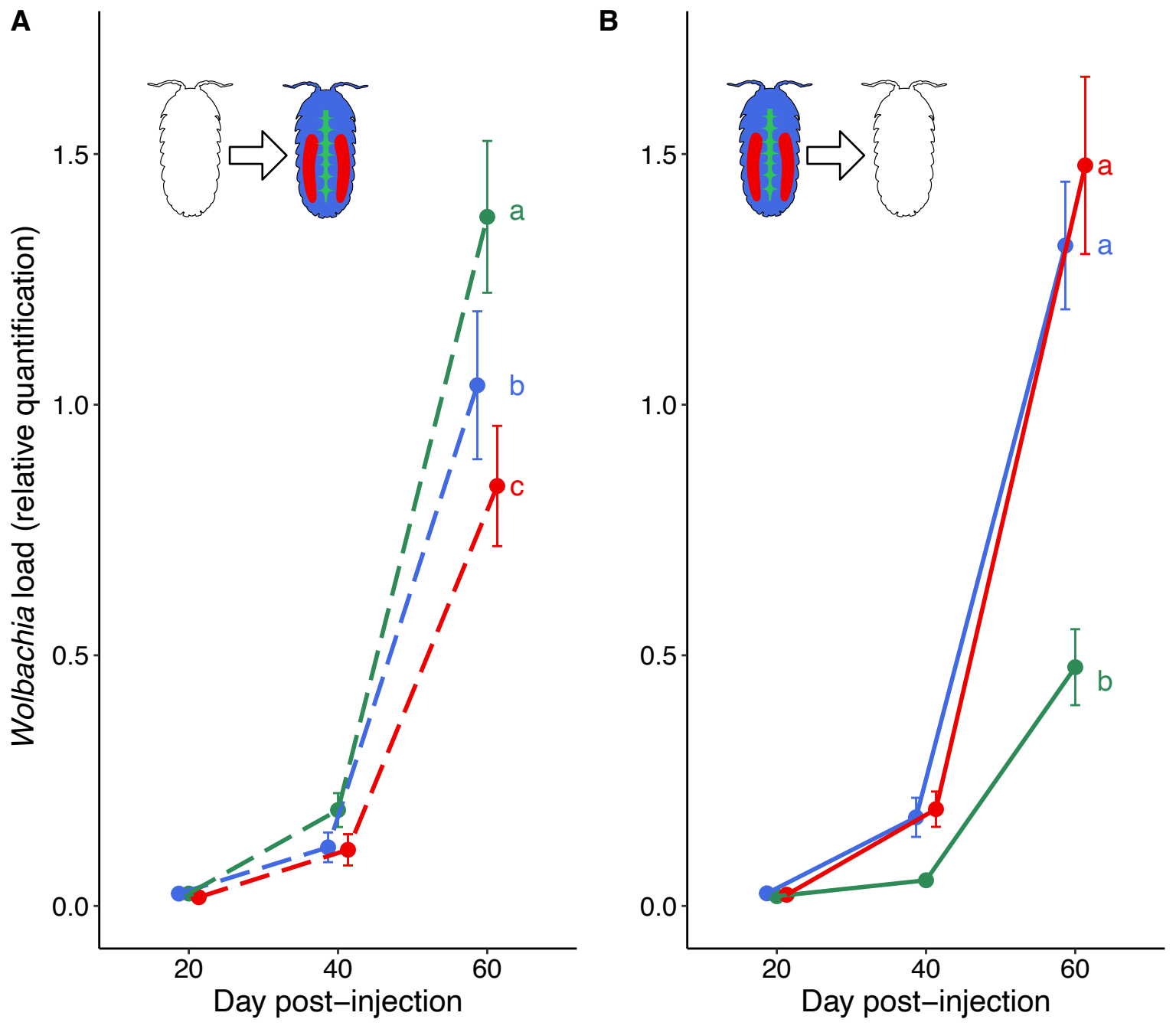
A
B
Wolbachia load (relative quantification)
1.5
1.0
0.5
0.0
20
40
60
Day post−injection
a
b
c
a
a
b

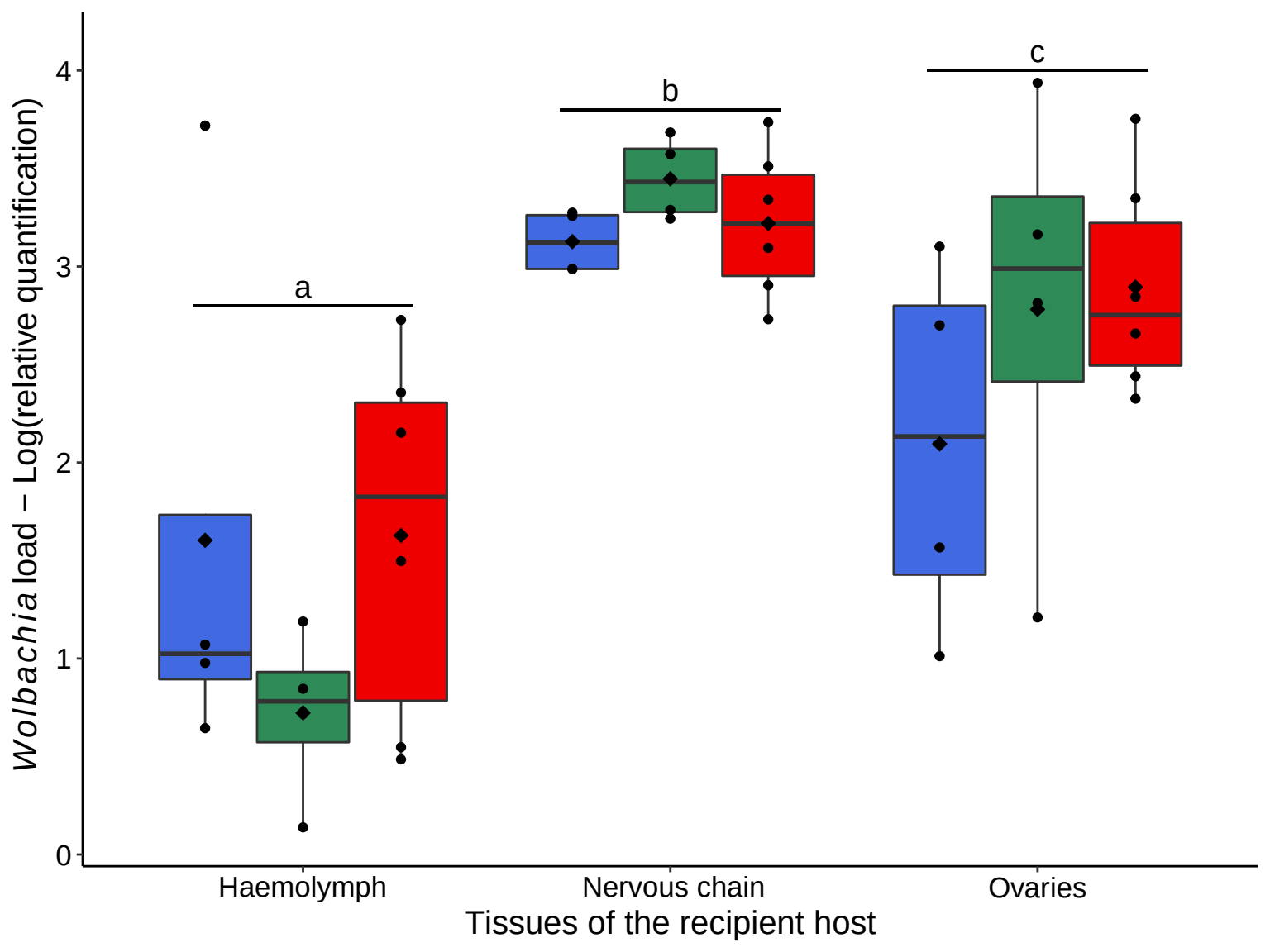
a
b
c
4
3
2
1
0
Wolbachia load – Log(relative quantification)
Haemolymph
Nervous chain
Ovaries
Tissues of the recipient host

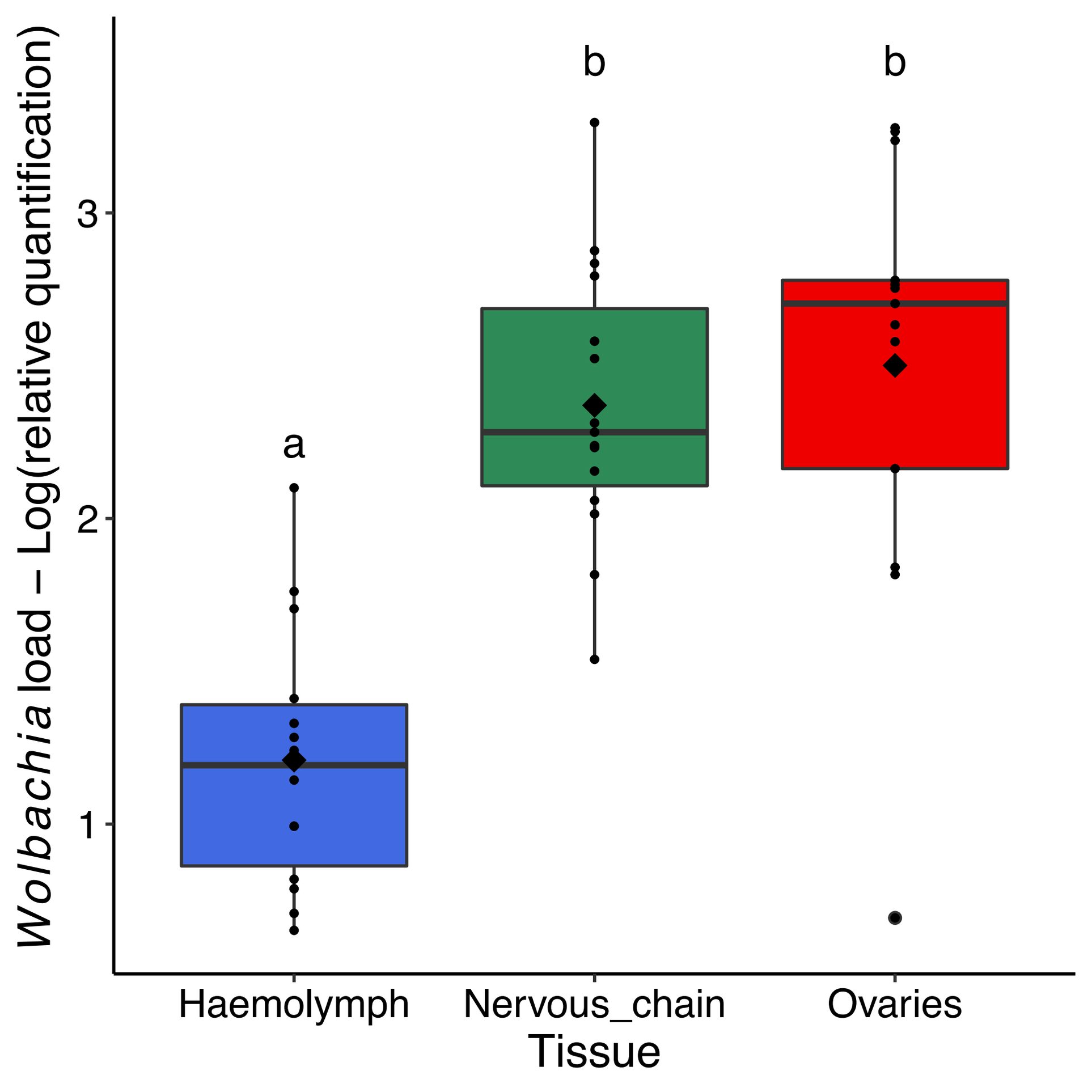
Wolbachia load – Log(relative quantification)
3
2
1
a
b
b
Haemolymph
Nervous_chain
Ovaries
Tissue

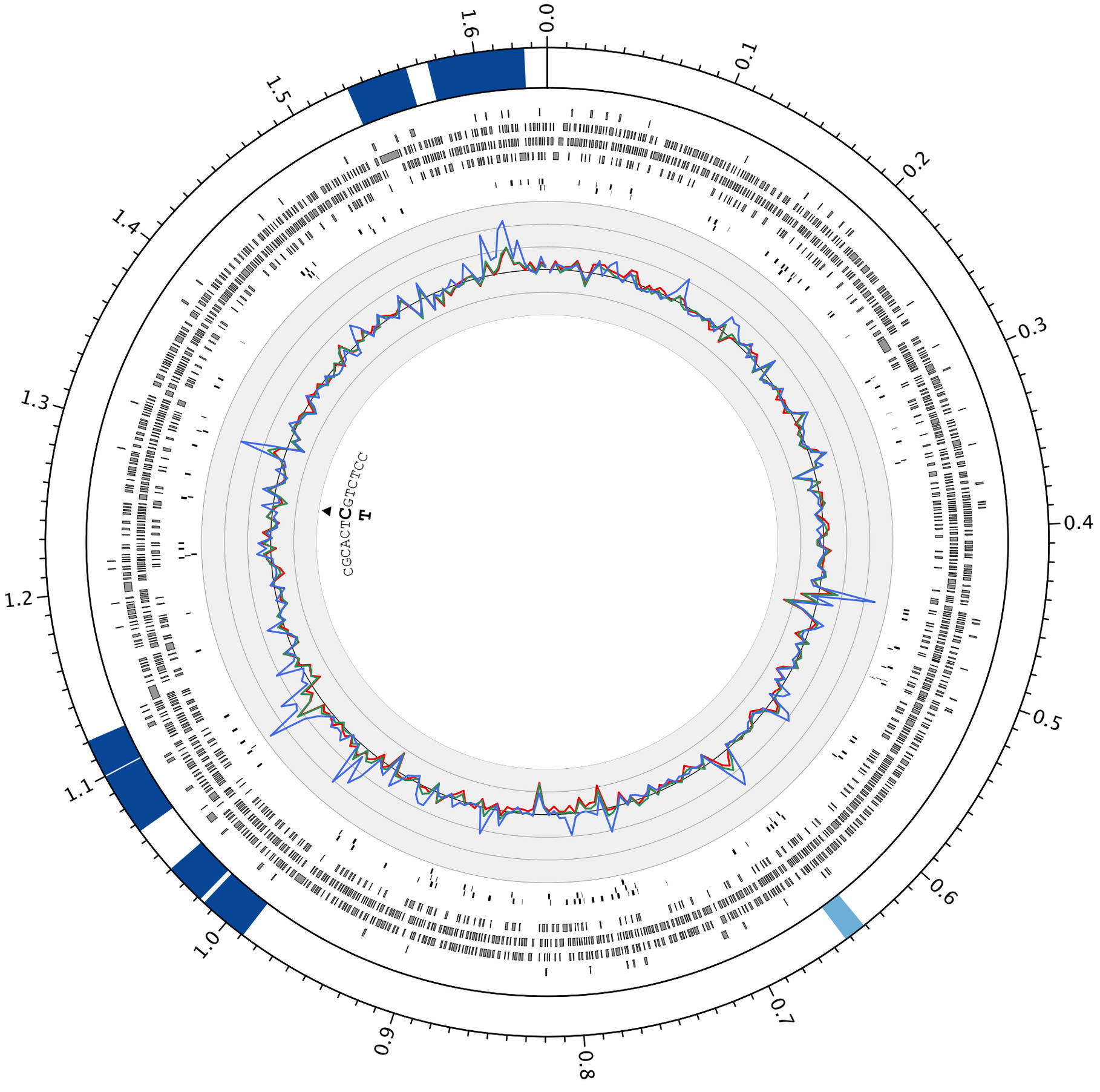
0.0
0.1
0.2
0.3
0.4
0.5
0.6
0.7
0.8
0.9
1.0
1.1
1.2
1.3
1.4
1.5
1.6
CGCACTCGTCTCC